Voltage-driven strain-mediated modulation of exchange bias in $Ir_{20}Mn_{80}/Fe_{80}Ga_{20}$/Ta/<011>-oriented PMN-32PT heterostructures

E. Demirci[1,*], J. de Rojas[1], A. Quintana[2], I. Fina[2], E. Menéndez[1], J. Sort[1,3,*]

[1]Departament de Física, Universitat Autònoma de Barcelona, 08193 Bellaterra, Spain

[2]Institut de Ciència de Materials de Barcelona (ICMAB-CSIC), Campus UAB, 08193 Barcelona, Spain

[3]Institució Catalana de Recerca i Estudis Avançats (ICREA), Pg. Lluís Companys 23, 08010 Barcelona, Spain

Abstract

Manipulation of exchange bias with electric field is appealing to boost energy efficiency in spintronic devices. Here, this effect is shown at room temperature in $Ir_{20}Mn_{80}/Fe_{80}Ga_{20}$/Ta layers grown onto <011>-oriented PMN-32PT single crystals. After magnetic field-cooling (FC) along the [01-1] and [100] in-plane directions of PMN-32PT and upon allowing the system to relax through consecutive hysteresis loops (training effect), the exchange bias field (H_{EB}) is measured under the action of voltage (out-of-plane poling). Depending on the applied voltage (magnitude and sign), H_{EB} can either increase or decrease with respect its value at 0 V. The relative variations of H_{EB} are 24% and 5.5% after FC along the [01-1] and [100] directions, respectively. These results stem from strain-mediated magnetoelectric coupling. The applied electric field causes changes in the coercivity and the squareness ratio of the films, suggesting a reorientation of the effective magnetic easy axis in $Fe_{80}Ga_{20}$. However, larger H_{EB} values are observed when the squareness ratio is lower. It is claimed that the effect of voltage is equivalent to an in-plane component of an applied magnetic field oriented perpendicular to the cooling field direction. Perpendicular in-plane magnetic fields have been shown to induce an increase of exchange bias in some ferromagnetic/antiferromagnetic systems due to partial recovery of the untrained antiferromagnetic state. Remarkably, here, this effect is directly induced with voltage, therefore enhancing energy efficiency.

*Corresponding authors: e.demirci@gtu.edu.tr (Erdem Demirci); Jordi.Sort@uab.cat (Jordi Sort)

Manipulation of the magnetic properties of materials with voltage (*i.e.*, converse magnetoelectric effect) has been proposed as an appealing strategy to boost energy efficiency in high-density memories and other information technology devices. By replacing magnetic field actuation (through the use of miniaturized electromagnets) with electric fields (created by external voltage), it is possible to drastically reduce Joule heating effects, thereby minimizing electric power dissipation[1–7]. Converse magnetoelectric actuation has been shown to be an effective means to tune the coercivity, saturation magnetization or squareness ratio (*i.e.*, effective magnetic anisotropy) of thin films, taking advantage of electric surface charging (or charge carrier modulation in ferromagnetic semiconductors)[8,9], magneto-ionic effects (voltage-driven ion motion)[10,11] or strain-mediated multiferroic coupling[12–14], when the magnetic films are grown in direct contact with piezoelectric or ferroelectric underlayers or substrates.

Of particular interest is the control of "exchange bias" with voltage. Exchange bias refers to the shift of the hysteresis loop (along the magnetic field axis) typically observed in exchange coupled ferromagnetic-antiferromagnetic bilayers. This effect constitutes the basis of spin valves and magnetic tunnel junctions employed in modern magnetic read heads and magnetic random-access memories (MRAMs). While there has been tremendous progress over the years in increasing the areal density of high-density hard disk drives, a bottleneck still exists in minimizing their overall power consumption. This problem is even more pronounced in large data servers, where almost 40% of the incoming powers is wasted in the form of heat dissipation[15]. Manipulation of exchange bias with voltage could contribute to face this energy efficiency challenge and could lead to next-generation voltage-controlled spintronic devices.

During the last few years, several strategies have been reported to control exchange bias with voltage[16]. First attempts included the use of single-phase magnetoelectric materials with simultaneous antiferromagnetic and ferroelectric properties, such as Cr_2O_3[17,18] (and B-doped Cr_2O_3[19]), $YMnO_3$[20]or $BiFeO_3$[21,22]. This led to the implementation of the first magnetoelectric MRAM architectures, although this approach is limited by the scarcity of single-phase antiferromagnetic multiferroic materials. Later, strain-mediated effects were used to tailor exchange bias (decreasing it by about 2.5%) in ferromagnetic Mn-Ni-Sn shape memory alloys grown onto ferroelectric substrates, such as $0.7Pb(Mg_{1/3}Nb_{2/3})O_3{-}0.3PbTiO_3$ (PMN−30PT), via martensitic phase transformations[23]. Somewhat larger changes were observed with voltage in CoFeB/IrMn and $[Co/Pt]_n$/IrMn multilayered films (with suitable seed layers) grown onto PMN−PT, but the effect of voltage was mostly to decrease (not increase) the loop shift compared to the pristine films with no voltage applied[24–26]. More prominent effects have been reported in exchange bias systems comprising a highly magnetostrictive layer in their structure (*e.g.*, FeGa), grown onto suitable

ferroelectric substrates, although reversibility problems have been identified[16,27]. Finally, very recently, a few works have reported on the possibility to also control exchange bias magneto-ionically in *e.g.* Co/FeO_x[28], Gd/$Ni_{1-x}Co_xO$[29] or NiO/Pd/Co/Pd/Gd$(OH)_3$/Au[30] thin films. However, a major challenge of magneto-ionics is the switching speed, which remains lower than for strain-mediated magnetoelectric systems[31,32].

One of the problems in assessing the effect of voltage on exchange bias is the occurrence of the so-called "training effect". This refers to the progressive decrease of the loop shift typically observed in some ferromagnetic/antiferromagnetic systems when consecutive hysteresis loops are recorded. The training effect has been ascribed to a relaxation of the interfacial antiferromagnetic spins configuration from an initial state with high antiferromagnetic interface magnetization (*i.e.*, after field cooling) to the equilibrium state with lower interfacial magnetization[33,34]. Training effects can mask the true voltage-dependence of exchange bias. The interplay between training effects and magnetoelectricity becomes even more intricate since it has been reported that voltage itself can induce a reset of the training effect, as seen, for example, in Cr_2O_3/CoPd multilayers[35]. This is in line with the possible influence of electric field on the anisotropy of some metallic antiferromagnetic materials[36].

In this work, we investigate voltage-control of exchange bias in IrMn/FeGa/Ta systems grown onto PMN−32PT. This particular ferroelectric substrate is selected because of its large piezoelectric coefficients for a composition near the morphotropic phase boundary and because of the highly asymmetric in-plane voltage-induced strains when out-of-plane poling is applied along the <011> direction[13,37]. We observe that, once the training effect is subtracted, voltage in this system can induce either an increase or a decrease of the exchange bias field with respect to the films with no voltage applied. Contrary to previous works on voltage-controlled exchange bias, which have mainly focused on the use of systems containing a magnetoelectric or multiferroic antiferromagnet (*e.g.*, Cr_2O_3 or $BiFeO_3$, where electric and magnetic orders directly influence each other or are mutually coupled), the mechanism explored here (*i.e.*, voltage-driven strain-mediated tuning of exchange bias through the use of an underlying ferroelectric substrate) can, in principle, be used as a universal way to tailor exchange bias. This makes our approach highly appealing because it is not limited to specific magnetoelectric/multiferroic antiferromagnetic layers.

$Ir_{20}Mn_{80}$(20nm)/$Fe_{80}Ga_{20}$(10nm)/Ta(10nm) thin films were grown by sputtering on ferroelectric <110>-oriented PMN−32PT single crystals (with thickness of 0.25 mm and area of 12 mm^2) in a vacuum chamber with a base pressure of 1×10^{-8} Torr by using an AJA International magnetron system. During sputtering, the working pressure was kept at 3×10^{-3} Torr. The 10 nm

Ta buffer layer inserted between $Fe_{80}Ga_{20}$ and PMN−32PT served as the top electrode to apply voltage across the ferroelectric substrate (as shown in Fig. 1(a)). For this, a tiny part (< 1 mm^2) of a corner of the Ta layer was physically masked. Upon deposition of $Fe_{80}Ga_{20}$ and $Ir_{20}Mn_{80}$, the mask was removed. The bottom electrode was made by uniformly covering the back side of PMN−32PT with silver paste. In this way, tunable electric fields were homogeneously applied across the ferroelectric PMN−32PT substrate by varying the strength of the applied voltage (*i.e.*, out-of-plane poling). To investigate converse magnetoelectric effects, hysteresis loops were recorded by vibrating sample magnetometry (VSM) from MicroSense while applying voltage *in-situ*. From each hysteresis loop, the values of coercivity, H_C (half width of the hysteresis loop), exchange bias field, H_{EB} (shift of the hysteresis loop along the magnetic field axis), and remanence-to-saturation ratio (squareness ratio), M_R/M_S (evaluated from centered loops, after correcting for the loop shift) were determined. Prior to magnetoelectric measurements, the sample was field-cooled to induce the unidirectional exchange coupling effect between the ferromagnetic ($Fe_{80}Ga_{20}$) and antiferromagnetic ($Ir_{20}Mn_{80}$) layers (*i.e.*, exchange bias). The field-cooling (FC) procedure consisted of first heating the sample to 400 K without magnetic field and then cooling it down to room temperature under H = 5 kOe external magnetic field. After FC, consecutive hysteresis loops were recorded in order to virtually eliminate training effects (*i.e.*, to get rid of the progressive reduction of exchange bias field upon repeated measurements). After 25 loops, the decrease of exchange bias for two consecutive loops was already below 1%. Subsequently, different DC voltage values, in the range from -200 V to +200 V, were applied. Hysteresis loops were measured along the FC direction. This procedure was repeated after FC along the [100] and [01-1] in-plane directions of the PMN−32PT substrate. The ferroelectric properties of PMN−32PT were determined using static polarization hysteresis loops measurements using the static mode of the TFAnalyser 2000 (aixACCT), with an integration time of 1 ms and relaxation time of 1 s. The ferroelectric polarization *vs*. electric field loop was collected by grounding one of the electrodes (silver paste) while biasing the other (Ta + silver paste). With this protocol, the displacive current flow through the circuit (*I*) was measured and the polarization *P* was obtained from the integrated current in time and normalized by the area (*A*): $P = 1/A \int I\mathrm{d}t + \mathrm{c}$. The constant "c" was selected to obtain a loop where the polarization values at maximum negative and positive applied voltage are equal. The used sign convention is the standard, *i.e.*, positive applied voltage corresponds to electric field pointing toward the grounded electrode.

The dependence of electric polarization (*P*) of PMN-32PT on the electric field (*E*) (ferroelectric hysteresis loop) in quasistatic conditions is shown in Fig. 1(b). The coercive electric field, saturation polarization and remanent polarization were determined to be 2.3 kV/cm, 8.2

μC/cm^2, and 5.1 μC/cm^2, respectively, at room temperature. Fig. 1(c) shows the square of the electric polarization as a function of electric field. Note that P^2 is proportional to the deformation that the PMN−32PT undergoes when subjected to the electric field due to its piezoelectric characteristics.

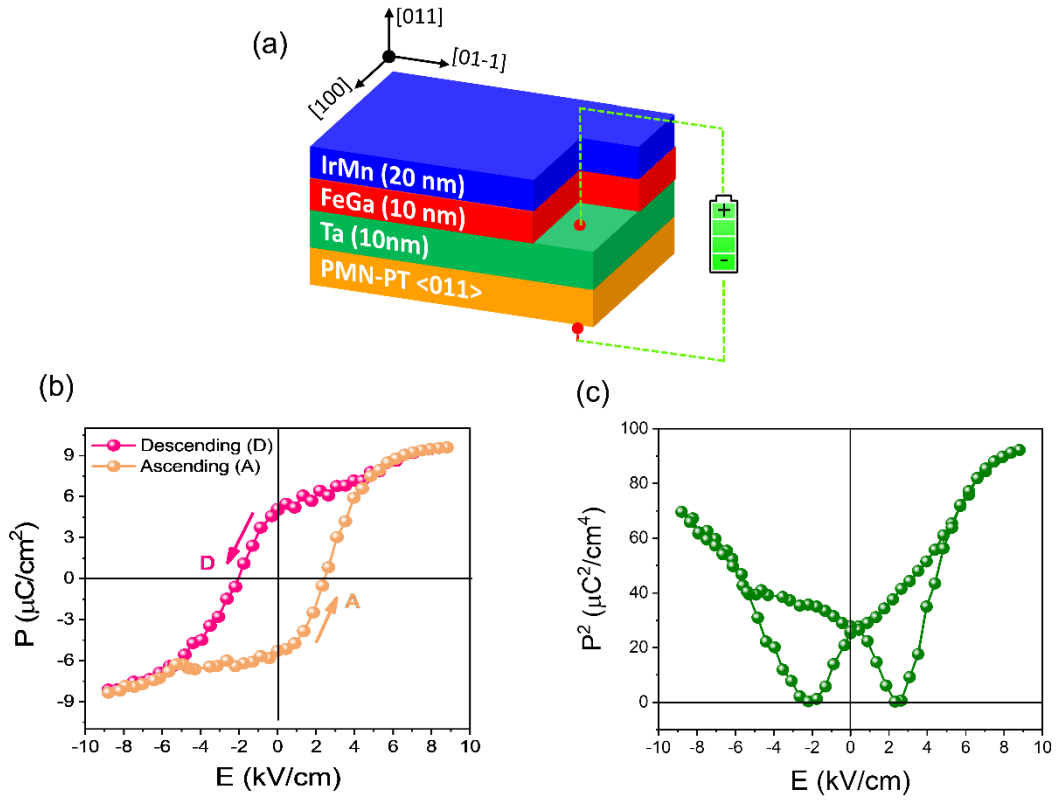

FIG. 1. (a) Schematic representation of the electric configuration used to apply voltage to the $Ir_{20}Mn_{80}/Fe_{80}Ga_{20}$/Ta/PMN−32PT system. (b) Electric polarization (*P*) *vs*. electric field (*E*) (*i.e.*, ferroelectric hysteresis loop) corresponding to the <011>-oriented PMN−32PT substrate. (c) Square of polarization (P^2) *vs*. *E* for the <011>-oriented PMN–32PT substrate. Note that A and D denote the ascending and descending branches of the ferroelectric hysteresis loop.

First, we focus on the voltage control of exchange bias along the [100] direction. After field cooling along this direction, successive magnetic hysteresis loops were acquired to assess the training effect (*i.e.*, the decrease of H_{EB} for consecutive loops) (see Fig. 2(a)). Such decrease of H_{EB} has been ascribed in the literature to a rearrangement of interfacial antiferromagnetic spins upon repeated cycling[38,39]. Subtracting the training effects (*i.e.*, starting from a trained state) allowed for the investigation of bare (*i.e.*, intrinsic) magnetoelectric effects.

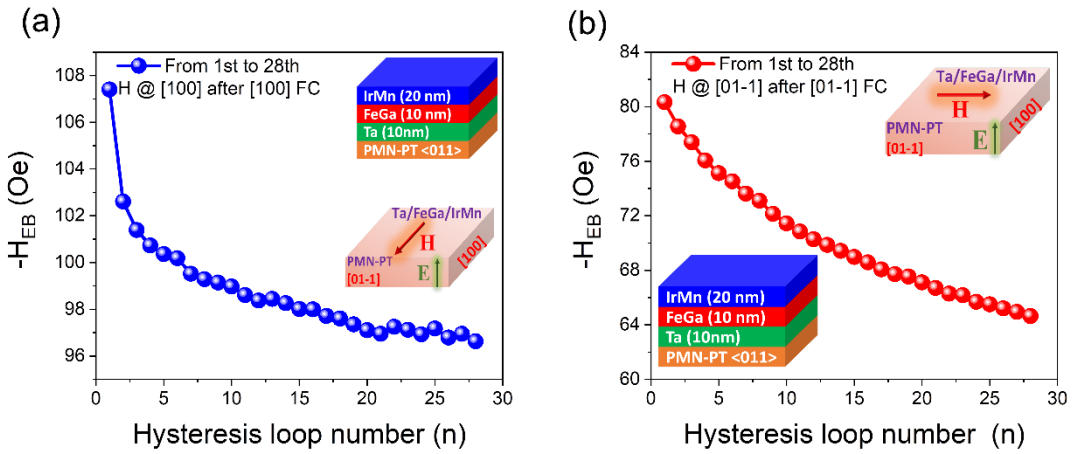

FIG. 2. Dependence of the loop shift H_{EB} (note that $-H_{EB}$ is plotted to show positive values) as a function of hysteresis loop number (training effect) measured upon successive hysteresis loops along the (a) [100] and (b) [01-1] in-plane directions.

After training effects levelled off, magnetic hysteresis loops were recorded along the [100] direction, under voltage, following the ascending (A) and descending (D) branches of the ferroelectric loop displayed in Fig. 1(b). The ferroelectric polarization at -8kV/cm was chosen as a starting reference point. The sample was always brought to this reference point before applying any other voltage value. Representative magnetic hysteresis loops corresponding to the as-grown state (before voltage application) and while applying +8 kV/cm (A) and -6 kV/cm (D) are shown in Fig. 3(a). These loops are always rather square, but slight changes in H_{EB}, H_C and M_R/M_S are observed as a function of voltage, as shown in Fig. 3(b,c,d). The overall dependences of H_C and M_R/M_S with voltage resemble those measured along the [100] direction on FeAl sputtered onto <110>-oriented PMN−32PT single crystals, ascribed to electric field-induced piezoelectric substrate deformation[13]. This is expectable since both FeAl and FeGa display similar magnetostrictive behavior[40]. Along the [100] direction, the relative variations of the magnetic properties with electric field are relatively small. For example, H_C changes by 7.5% whereas H_{EB} only by approximately 5.5% when comparing the extreme values. Nevertheless, it is remarkable that at 0 V H_{EB} is higher after voltage has been applied (*i.e.*, at ferroelectric remanence) than for the as-prepared sample (Fig. 3(b)). It is also worth mentioning that the smallest values of H_{EB} are observed at high positive voltages, when M_R/M_S becomes maximum. This is the opposite of what one might expect, since, in a first approximation, H_{EB} should be maximized when the FM anisotropy easy axis is parallel to the direction of antiferromagnetic interfacial spins (*i.e.*, the FC direction)[41]. So, this simple reasoning is not adequate to account for the magnetoelectric trends obtained in our case.

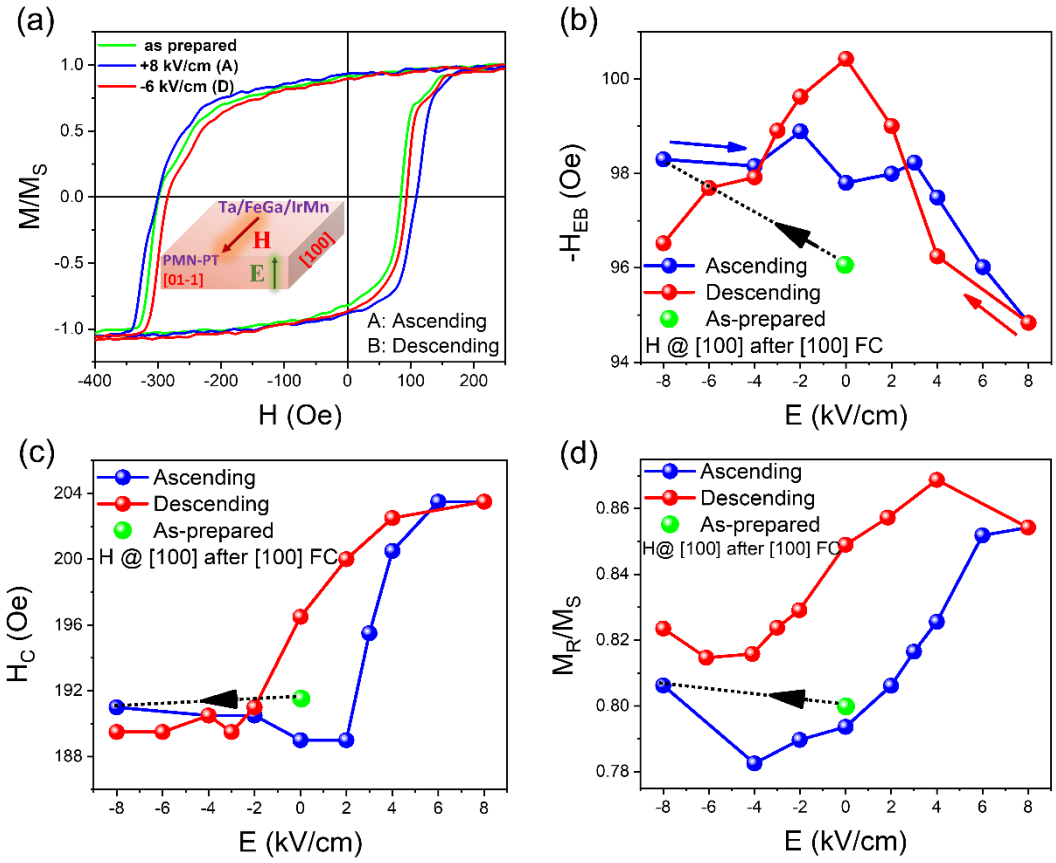

FIG. 3. Electric-field control of the magnetic properties in a $Ir_{20}Mn_{80}/Fe_{80}Ga_{20}$/Ta/PMN−32PT multilayer heterostructure after FC and measuring hysteresis loops under voltage along the [100] direction of the PMN−32PT substrate. Panel (a) shows representative hysteresis loops corresponding to selected values of the electric field. Panels (b), (c) and (d) show the dependence of the loop shift (H_{EB}), coercivity (H_C) and squareness ratio (M_R/M_S) on the electric field, respectively.

We also measured magnetoelectric effects along the [01-1] direction. The sample was again subjected to a FC process (along [01-1]) and successive hysteresis loops were recorded to assess the training effect along this direction (Fig. 2(b)). Representative hysteresis loops of the sample before voltage application and for selected values of electric field are shown in Fig. 4(a). The hysteresis loops of the as-prepared sample measured at 0 V along the [100] and [01-1] in-plane directions show some differences, particularly in the values of H_C and H_{EB}, which are clearly smaller along [01-1] (Fig. 3(a)). This suggests that FeGa exhibits some in-plane anisotropy after the sputtering and FC processes. Interestingly, when voltage is applied (always out-of-plane poling), larger variations in H_{EB} are observed along the [01-1] direction (up to 24%), compared to previous measurements along [100] (5.5%). While H_C changes only by 8.5% (not much larger than along the [100] direction), the variation of M_R/M_S with electric field is much more significant, from 0.9 to 0.55.

This is evident in the titled shape of the hysteresis loop corresponding to +4 kV/cm in Fig. 4(a). The overall shape of the M_R/M_S *vs*. *E* curve along the [01-1] direction is very similar to that reported for FeAl grown onto PMN−32PT[13]. In this case, M_R/M_S exhibits a clear loop-like shape where the magnetic properties switch from an easy to a hard axis behavior when the voltage polarity changes from negative to positive values. It has been claimed that the highly dissimilar magnetoelectric behaviors along the [100] and [01-1] directions of <011> substrates are due to the specific symmetry-related ferroelectric response of PMN−32PT around the morphotropic phase boundary, which leads to dissimilar piezoelectric coefficients along orthogonal in-plane directions (*e.g.*, $d_{31} \approx$ -2740 pm/V; $d_{32} \approx$ 1100 pm/V)[37]. Indeed, the variation of interplanar distance with voltage along the [01-1] direction is much more pronounced than along [100][13]. This additional stress-induced anisotropy along the [01-1] direction results from polarization reversal through formation of so-called 109° domain walls. In fact, ferroelectric switching in this material can take place via nucleation and domain wall movements of 71°, 109° and 180° domain walls. Domain walls of 180° and 71° imply a polarization reversal which occurs in a single [111] plane. Conversely, 109° domain walls lead to a 90° twist of the polarization (*P* rotates out of the plane of the domain wall), giving rise to a significant in-plane distortion along [01-1][42]. The higher strains along this direction promote larger variations in M_R/M_S compared to the less strained [100] direction.

Remarkably, similar to the [100] direction, the largest H_{EB} values along [01-1] (about 16.5% higher than in the as-prepared sample) are obtained under applied voltages rendering the lowest M_R/M_S values. This is counter-intuitive since squarer hysteresis loops (with FM anisotropy easy axis parallel to the FC direction) usually lead to larger H_{EB}. We believe this anomalous behavior is related to the training effect. It has been reported that, in FM-AFM bilayers exhibiting training effects, a perpendicular in-plane magnetic field causes an increase of H_{EB} due to induced changes in the alignment between the ferromagnetic magnetization and the uncompensated spins in the AFM layer[43]. In our work, we do not apply a perpendicular in-plane magnetic field, but the voltage causes a similar effect: part of the magnetization rotates away from [01-1] direction (*i.e.*, there is a component of the magnetization perpendicular to [01-1], thereby reducing M_R/M_S) and such an effect may partially re-establish the initial AFM configuration, thus increasing H_{EB}. We observe a more pronounced effect when the decrease of M_R/M_S is larger (*i.e.*, when the perpendicular component of the FM magnetization is larger).

It is worthwhile mentioning that previous works using Cr_2O_3 layers for the voltage-control of exchange bias[17] suffered from the limitation that the tuning of H_{EB} required of both an applied voltage and a heating and magnetic field cooling process through the Néel temperature of Cr_2O_3. In

our work, we can tune exchange bias with voltage directly at room temperature, without any need of heat treatments, which are detrimental in terms of energy efficiency.

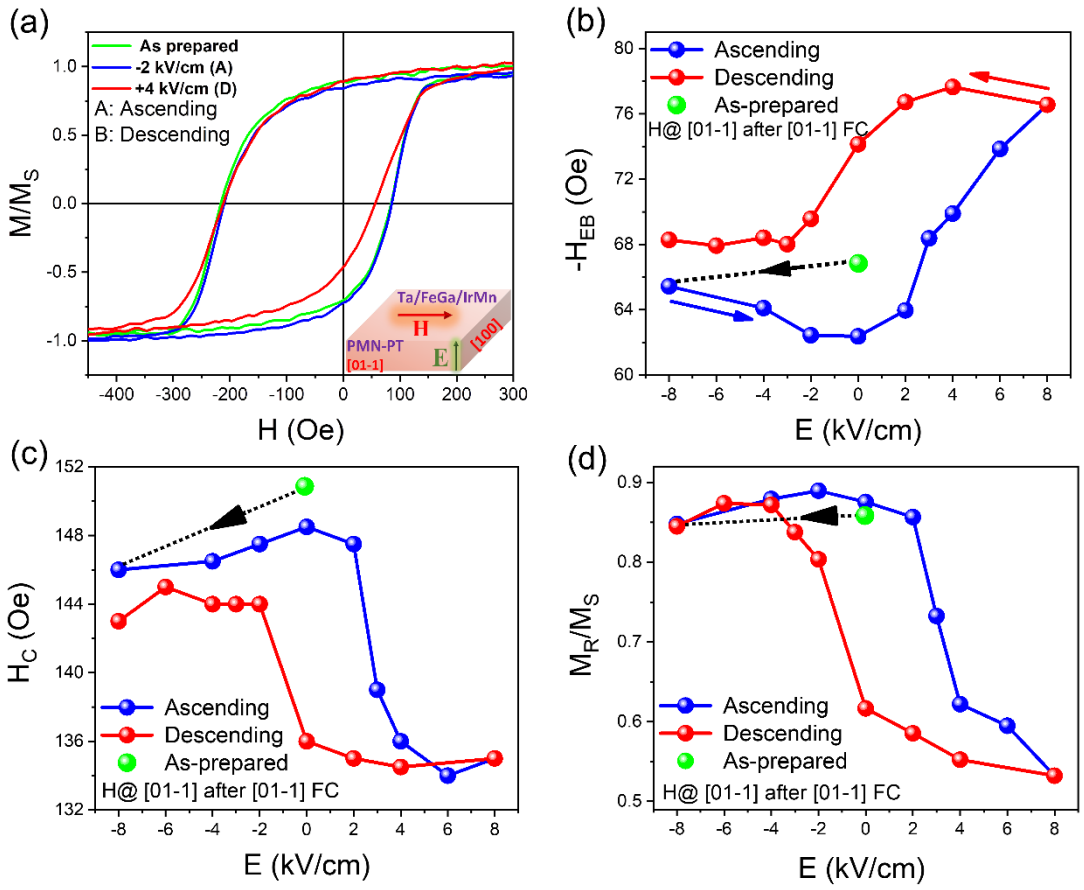

FIG. 4. Electric-field control of the magnetic properties in a $Ir_{20}Mn_{80}/Fe_{80}Ga_{20}$/Ta/PMN−32PT multilayer heterostructure after FC and measuring hysteresis loops under voltage along the [01-1] direction of the PMN–32PT substrate. Panel (a) shows representative hysteresis loops corresponding to selected values of the electric field. The dependence of the loop shift (H_{EB}), coercivity (H_C) and squareness ratio (M_R/M_S) on the electric field are shown in panels (b), (c) and (d), respectively.

In summary, the influence of an applied electric field on the exchange bias properties of $Ir_{20}Mn_{80}/Fe_{80}Ga_{20}$/Ta multilayer thin films grown onto ferroelectric <011>-oriented PMN–32PT single crystals has been investigated. After measuring and subtracting the effect of training, clear differences are observed in H_{EB} and M_R/M_S depending on the in-plane measurement direction. The largest variations in H_{EB} are found along the [01-1] direction (with an up to 24% change in H_{EB}, including an increase of 16.5% with respect to the sample before voltage application). The effect is attributed to strain-mediated magnetoelectric coupling. The externally applied voltage induces a reorientation of the FeGa magnetic easy axis, causing a strong decrease in M_R/M_S. This reorientation indicates that, for this substrate orientation, external out-of-plane voltage is

equivalent to applying an in-plane magnetic field perpendicular to the FC direction (which has been reported to cause an increase of H_{EB} due to partial recovery of the initial interfacial uncompensated AFM spins configuration). In our case, such an increase of H_{EB} can be directly induced by means of electric field in an energy efficient manner, *i.e.,* without the detrimental Joule heating effect that occurs in the electromagnets used to generate magnetic fields. Our results demonstrate an effective magnetoelectric control of exchange bias via strain, and are therefore appealing for the development of future low-power spintronic devices and magnetic sensors. In particular, the reported strain-mediated exchange bias bilayers could be integrated in advanced magnetoelectric random-access memories (ME-RAMs). The energy consumption in such type of strain-controlled ME-RAMs could be as low as a few aJ/switching event, which is several orders of magnitude lower than in conventional magnetoresistive MRAMs or spin-transfer-torque MRAMs, according to theoretical estimations reported during the last few years[44,45].

Acknowledgements

This work was supported by TÜBİTAK (The Scientific and Technological Research Council of Turkey) through the project number 1059B192000016. Partial financial support by the European Research Council (MAGIC-SWITCH 2019-Proof of Concept Grant, Agreement Nº 875018), the European Union's Horizon 2020 research and innovation programme (European Training Network, ETN/ITN Marie Skłodowska-Curie, Agreement Nº 861145), the Spanish Government (Severo Ochoa FUNFUTURE –CEX2019-000917-SMCIN, AEI/10.13039/501100011033–, MAT2017-86357-C3-1-R, PID2019-107727RB-I00, PID2020-116844RB-C21 and PDC2021-121276-C31), the Generalitat de Catalunya (2017-SGR-292) and the European Regional Development Fund (MAT2017-86357-C3-1-R) is acknowledged. E.M. is a Serra Húnter Fellow. A. Quintana acknowledges the Spanish Ministry of Science, Innovation and Universities for the Juan de la Cierva Formación contract (FJC2019-039780-I).

REFERENCES

[1] X. Liang, H. Chen, and N.X. Sun, APL Mater. **9**, 041114 (2021).

[2] Z. Chu, C. Dong, C. Tu, X. Liang, H. Chen, C. Sun, Z. Yu, S. Dong, and N.-X. Sun, Appl. Phys. Lett.

115, 162901 (2019).

[3] G. Sreenivasulu, U. Laletin, V.M. Petrov, V. V Petrov, and G. Srinivasan, Appl. Phys. Lett. **100**, 173506 (2012).

[4] T. Nan, H. Lin, Y. Gao, A. Matyushov, G. Yu, H. Chen, N. Sun, S. Wei, Z. Wang, M. Li, X. Wang, A. Belkessam, R. Guo, B. Chen, J. Zhou, Z. Qian, Y. Hui, M. Rinaldi, M.E. McConney, B.M. Howe, Z. Hu, J.G. Jones, G.J. Brown, and N.X. Sun, Nat. Commun. **8**, 296 (2017).

[5] C. Navarro-Senent, A. Quintana, E. Menéndez, E. Pellicer, J. Sort, APL Mater. **7**, 030701 (2019).

[6] T. Kosub, M. Kopte, R. Hühne, P. Appel, B. Shields, P. Maletinsky, R. Hübner, M.O. Liedke, J. Fassbender, O.G. Schmidt, and D. Makarov, Nat. Commun. **8**, 13985 (2017).

[7] C. Tu, C. Dong, Z. Chu, H. Chen, X. Liang, and N.X. Sun, Appl. Phys. Lett. **113**, 262904 (2018).

[8] H. Ohno, D. Chiba, F. Matsukura, T. Omiya, E. Abe, T. Dietl, Y. Ohno, and K. Ohtani, Nature **408**, 944 (2000).

[9] D. Chiba, A. Werpachowska, M. Endo, Y. Nishitani, F. Matsukura, T. Dietl, and H. Ohno, Phys. Rev. Lett. **104**, 106601 (2010).

[10] A.J. Tan, M. Huang, C.O. Avci, F. Büttner, M. Mann, W. Hu, C. Mazzoli, S. Wilkins, H.L. Tuller, G.S.D. Beach, Nat. Mater. **18**, 35 (2019).

[11] J. de Rojas, A. Quintana, A. Lopeandia, J. Salguero, B. Muíz, F. Ibrahim, M. Chshiev, A. Nicolenco, M.O. Liedke, M. Butterling, A. Wagner, V. Sireus, L. Abad, C. J. Jensen, K. Liu, J. Nogués, J.L. Costa-Krämer, E. Menéndez, and J. Sort, Nat. Commun. **11**, 5871 (2020).

[12] I. Fina, A. Quintana, J. Padilla-Pantoja, X. Martí, F. Macià, F. Sánchez, M. Foerster, L. Aballe, J. Fontcuberta, J. Sort, ACS Appl. Mater. Interfaces **9**, 15577 (2017).

[13] E. Menéndez, V. Sireus, A. Quintana, I. Fina, B. Casals, R. Cichelero, M. Kataja, M. Stengel, G. Herranz, G. Catalán, M.D. Baró, S. Suriñach, and J. Sort, Phys. Rev. Appl. **12**, 14041 (2019).

[14] M. Liu, O. Obi, J. Lou, Y. Chen, Z. Cai, S. Stoute, M. Espanol, M. Lew, X. Situ, K.S. Ziemer, V.G. Harris, and N.X. Sun, Adv. Funct. Mater. **19**, 1826 (2009).

[15] N. Jones, Nature **561**, 163 (2018).

[16] Q. Yang, Z. Zhou, N.X. Sun, and M. Liu, Phys. Lett. A **381**, 1213 (2017).

[17] P. Borisov, A. Hochstrat, X. Chen, W. Kleemann, and C. Binek, Phys. Rev. Lett. **94**, 117203 (2005).

[18] X. Chen, A. Hochstrat, P. Borisov, and W. Kleemann, Appl. Phys. Lett. **89**, 202508 (2006).

[19] M. Street, W. Echtenkamp, T. Komesu, S. Cao, P.A. Dowben, and C. Binek, Appl. Phys. Lett. **104**, 222402 (2014).

[20] V. Laukhin, V. Skumryev, X. Marti, D. Hrabovsky, F. Sánchez, M. V Garcia-Cuenca, C. Ferrater, M. Varela, U. Lüders, J.F. Bobo, and J. Fontcuberta, Phys. Rev. Lett. **97**, 227201 (2006).

[21] S.M. Wu, S.A. Cybart, P. Yu, M.D. Rossell, J.X. Zhang, R. Ramesh, and R.C. Dynes, Nat. Mater. **9**, 756 (2010).

[22] M. Bibes and A. Barthélémy, Nat. Mater. **7**, 425 (2008).

[23] Q. Xie, Y. Ma, X. Zhang, L. Wang, G. Yue, and D.-L. Peng, J. Alloys Compd. **619**, 235 (2015).

[24] S. Rizwan, G.Q. Yu, S. Zhang, Y.G. Zhao, and X.F. Han, J. Appl. Phys. **112**, 64120 (2012).

[25] A. Chen, Y. Zhao, P. Li, X. Zhang, R. Peng, H. Huang, L. Zou, X. Zheng, S. Zhang, P. Miao, Y. Lu, J. Cai, and C.-W. Nan, Adv. Mater. **28**, 363 (2016).

[26] E. Song, Z. Guo, G. Li, F. Liao, G. Li, H. Du, O.G. Schmidt, M. Kim, Y. Yi, W. Bao, and Y. Mei, Adv. Electron. Mater. **5**, 1900232 (2019).

[27] M. Liu, J. Lou, S. Li, and N.X. Sun, Adv. Funct. Mater. **21**, 2593 (2011).

[28] L. Wei, J. Qu, R. Zheng, R. Liu, Y. Yuan, J. Wang, L. Sun, B. You, W. Zhang, Q. Xu, and J. Du, AIP Adv. **10**, 15306 (2020).

[29] P.D. Murray, C.J. Jensen, A. Quintana, J. Zhang, X. Zhang, A.J. Grutter, B.J. Kirby, and K. Liu, ACS Appl. Mater. Interfaces **13**, 38916 (2021).

[30] J. Zehner, D. Wolf, M.U. Hasan, M. Huang, D. Bono, K. Nielsch, K. Leistner, and G.S.D. Beach, Phys. Rev. Mater. **5**, L061401 (2021).

[31] J.M. Hu and C.W. Nan, APL Mater. **7**, (2019).

[32] X. Liang, A. Matyushov, P. Hayes, V. Schell, C. Dong, H. Chen, Y. He, A. Will-Cole, E. Quandt, P. Martins, J. McCord, M. Medarde, S. Lanceros-Méndez, S. van Dijken, N.X. Sun, and J. Sort, IEEE Trans. Magn. **57**, 1 (2021).

[33] C. Binek, Phys. Rev. B **70**, 14421 (2004).

[34] E. Menéndez, T. Dias, J. Geshev, J.F. Lopez-Barbera, J. Nogués, R. Steitz, B.J. Kirby, J.A. Borchers, L.M.C. Pereira, A. Vantomme, and K. Temst, Phys. Rev. B **89**, 144407 (2014).

[35] W. Echtenkamp and C. Binek, Phys. Rev. Lett. **111**, 187204 (2013).

[36] Y. Wang, X. Zhou, C. Song, Y. Yan, S. Zhou, G. Wang, C. Chen, F. Zeng, and F. Pan, Adv. Mater. **27**, 3196 (2015).

[37] Y. Lu, D.-Y. Jeong, Z.-Y. Cheng, Q.M. Zhang, H.-S. Luo, Z.-W. Yin, and D. Viehland, Appl. Phys. Lett. **78**, 3109 (2001).

[38] E. Demirci, M. Öztürk, E. Sınır, U. Ulucan, N. Akdoğan, O. Öztürk, and M. Erkovan, Thin Solid Films **550**, 595 (2014).

[39] H. Fulara, S. Chaudhary, and S.C. Kashyap, Appl. Phys. Lett. **101**, 142408 (2012).

[40] J.R. Cullen, A.E. Clark, M. Wun-Fogle, J.B. Restorff, and T.A. Lograsso, J. Magn. Magn. Mater. **226**–**230**, 948 (2001).

[41] J. Nogués and I.K. Schuller, J. Magn. Magn. Mater. **192**, 203 (1999).

[42] P. Marton, I. Rychetsky, and J. Hlinka, Phys. Rev. B **81**, 144125 (2010).

[43] S. Brems, K. Temst, and C. Van Haesendonck, Phys. Rev. Lett. **99**, 67201 (2007).

[44] J.-M. Hu and C.-W. Nan, APL Mater. **7**, 080905 (2019).

[45] H. Cai, W. Kang, Y. Wang, L. A. de Barros Naviner, J. Yang, and W. Zhao, Appl. Sci. **7**, 929 (2017).